Bioconjugate Chemistry

ARTICLE

pubs.acs.org/bc

FRET-Based Biosensor for Oleic Acid in Nanomolar Range with Quantum Dots As an Energy Donor

Sergey V. Dezhurov,* Irina Y. Volkova, and Maxim S. Wakstein

Applied Acoustics Research Institute, Moskow region, Dubna, Russia

Supporting Information

ABSTRACT: A self-assembling sensor for oleic acid has been developed. The sensor consists of a self-assembling fluorescent dye labeled BSA and quantum dots CdSe/ZnS capped with 3-mercaptopropionic acid. The detection limit of the new sensor is 10−1000 nM. The influence of the quantum dot size on the FRET efficiency in the course of the interaction of the sensor system with the analyte has been studied. The pH dependence, aggregation stability. and electrophoretic properties of the sensor have been examined. The data suggest a new approach for the development of nanoscale FRET-based sensors operating effectively due to unique fluorescent properties of quantum dots as well as due to selective protein−ligand interactions.

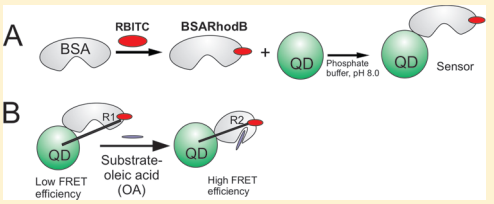

INTRODUCTION

One of the most important tasks in sensor technology is to create highly selective, fast, and sensitive tools for the detection of specific analytes. Among others, fluorescent detection techniques possess the advantages of versatility, high sensitivity, and the simplicity of signal detection.[1] Versatility is ensured not only by the possibility to choose the type of a sensor but also by a variety of different approaches for signal registration including fluorescence microscopy, flow fluorocytometry, and single photon counting methods among others. Moreover, considerable achievements in the production of highly stable and bright fluorophores based on semiconductor quantum dots (QDs) have already led to the development of a variety of nanoscale sensors.[2−5] Meanwhile, the problems of complicated synthetic chemistry (the synthesis of aptamers,[3] polypeptides, and organic compounds[2,4]) as well as multistage procedures for sensor production still limit their wide application.

The most widely spread detection systems relying on the fluorescent response are Förster resonance energy transfer (FRET)-based sensors.[1,6] FRET has provided researchers with a powerful tool to probe a variety of biological processes. These include protein−protein interactions, ligand−receptor binding, and changes in protein and oligonucleotide conformation in response to biological substrates.[6]

The promising application of the FRET-systems is the development of nanoscale bio sensors.[2−7] In this case, one of the best choices of donors (Ds) is quantum dots (QDs) due to their unique, easily tunable optical properties and due to their ability of non covalent self-assembly with proteins.[8−12] The fluorescent dyes or proteins are usually used as acceptors (As).[5] As a rule, the FRET effectiveness of such systems changes either after the association/dissociation of complexes or as a response to chemical transformations of molecules, both of which lead to a considerable change in the distance (r) between D and A.[4] The possibility of studying specific interactions by monitoring small shifts of the parameters r and/or orientation factor (κ) as a result of local changes in A:D complex was also demonstrated that.[13] Since the synthesis scheme of QDs makes it possible to vary the parameter r depending on the size of QDs and Förster radius (R_0) depending on the integral overlapping of emission spectrum of D and the absorption spectrum of A, it is possible to create systems with high sensitivity to even small conformational changes in the system. Thus, the main purpose of this study was to confirm the possibility of creating an adjustable sensing system based on the tunable properties of QDs.

To this end, a simple approach to the formation of sensor complexes based on the self-assembly of rhodamine B (Rhod B)-labeled bovine serum albumin with 3-mercaptopropionic acid (MPA) coated CdSe/ZnS QDs is suggested. The model system is sensitive to oleic acid (in the concentration range from 10 to 1000 nM), which is the native ligand of BSA. The optimal configuration for the system is achieved by the variation of the parameters r and R_0. The former is influenced by the QD diameter while the latter by the integral spectral overlap of donors having different emission wavelengths (emission maxima between 520 and 550 nm) and the quantum yield of the donor (QYD).

The QD−BSA complexes suggested in this study are promising tools for the diagnosis of hypertension, microangiopathy, and insulin resistance, which are pathologies, resulting from the increased level of free fatty acids in plasma.[14−17] The relevance of fatty acid determination is also connected with their significant contribution to the progression of incidents of metabolic

Received: March 11, 2010
Revised: January 25, 2011
Published: February 18, 2011

disorders.[18] To date, there are sensors for fatty acids based on FRET between a dye and Ru-complex,[19] as well as on chromatographic methods.[20−22] Liquid chromatography (LC-MS) has a limit of detection for fatty acid in the femtomolar range,[22] which is one of the highest sensitivity achieved for the analyte. However, the application of LC-MS is limited by low productivity, high cost, and complexity, due to the need for sample preparation and derivatization procedures. The sensor developed in our laboratory has sensitivity close to that reported for the FRET system.[19] Despite the fact that this approach is 3 orders of magnitude less sensitive than LC-MS, the method suggested herein is rapid, convenient, and easy to use.

EXPERIMENTAL PROCEDURES

Instruments and Materials. Oleic acid 99%, cadmium oxide 99.99+% (Alfa), 1-octadecene (OD) 90%, oleylamine (OLA) 70%, zinc acetate 99.99%, rhodamine B isothiocyanate (RBITC), hexamethyldisilathiane (HMDST), and coumarin 1 99% were purchased from Aldrich. Trioctylphosphine (TOP) 99%, trioctylphosphine oxide (TOPO) 90%, hexadecylamine (HDA) 99%, 3-mercaptopropionic acid (MPA) 99% (Fluka), selenium 99.9% (Merck), 1-butanol 99.8%, methanol 99%, and rhodamine 6G 99% were purchased from Acros. Tris(hydroxymethyl)aminomethane 99.9%, bovine serum albumin (BSA), and glycine 99% were purchased from MP Biochemicals. Agarose electrophoretic grade was purchased from BioRad. Activated carbon, chloroform, hexane, toluene, NaOH, Na_2HPO_4, and phosphoric acid were chemically pure. Ultracentrifugation tubes (50 kDa MWCO) were purchased from Millipore. PES syringe filters (0.22 μm) and PD-10 columns were purchased from GE Healthcare.

Fluorescence measurements were carried out using a Cary Eclipse (Varian) spectrofluorometer. Absorption spectra were recorded using a Cary 100 (Varian) spectrophotometer. Determination of hydrodynamic sizes of particles was performed using Nanotrac Ultra (Microtrac). Agarose gel experiments were performed in Tris−glycine buffer at a constant voltage of 90 V at room temperature in a horizontal electrophoresis unit (Bio-Rad).

Synthesis of Water-Soluble CdSe/ZnSMPA QDs. Hydrophobic CdSe/ZnS QDs were synthesized in accordance with an earlier developed protocol[23] with some modifications.

Synthesis of CdSe Core Nanocrystals. Cadmium oleate (0.2 mmol), HDA (0.2 mmol), OLA (0.9 mmol), and 10 mL of OD were added into a 50 mL three-necked flask and were kept in vacuo for one hour at 100 °C. The mixture was then heated to 160−200 °C (depending on the required size of the QDs) under Ar flow, and 1 mL of 2 M TOPSe solution was quickly injected with a syringe. The reaction was stopped after 10−300 s by the injection of cooled hexane (10 mL). The reaction mixture was diluted with 10 mL of toluene and 10 mL of butanol. The nanocrystals were precipitated with methanol until the solution became visually turbid. The mixture was centrifuged until the particles were fully precipitated. The precipitate was redispersed in 6 mL of hexane/butanol/toluene mixture (1:1:1) and was reprecipitated with methanol as described above. The precipitation procedure was repeated 3 times. The obtained precipitate of CdSe QDs was dissolved in 5 mL of hexane and centrifuged in order to remove aggregates. The concentration of QDs was estimated spectrophotometrically.[24]

Synthesis of CdSe/ZnS Core/Shell Nanocrystals. The CdSe QDs solution (~0.1 μmol) was injected into the mixture of 2 g of HDA and 4 g of TOPO at 180 °C under Ar and stirred. For covering CdSe cores with 1−2 monolayers of ZnS (depending on the demanded emission wavelength), 0.2 M of zinc acetate in OD:OLA 3:1 was injected after the temperature returned to the original value. The quantities of the Zn and S precursors were calculated as described elsewhere.[23] At the next stage, an equal amount of HMDST was added dropwise. After that, the mixture was kept for 30 min at 180 °C and then cooled. CdSe/ZnS QDs were isolated from the reaction mixture in the same way as the CdSe core nanocrystals. Finally, nanocrystals were dissolved in $CHCl_3$ to a concentration of 10 μM.

Surface Modification with MPA. The solution of hydrophobic QDs in $CHCl_3$ was cooled under Ar to 0 °C. The solution of MPA (1 M) in $CHCl_3$ was injected via a septum to a final concentration of 0.13 M, and the mixture was stirred at 0 °C for one hour. Then the QDs were precipitated with NH_3 saturated methanol (1:1 v/v). The precipitate was isolated by centrifugation, washed with diethyl ether, and dried under vacuum. After that, the QDs were dispersed in 25 mM phosphate buffer. A small amount of aggregates (less than 5 wt %) were removed by centrifugation and filtration through the 0.22 μm membrane filter. The concentration of the QDs was estimated spectrophotometrically.[24] The fluorescence quantum yield of the QDs was determined as described earlier[25] using coumarin 1 as a standard.

The synthesis of water-soluble CdSe/ZnSMPA QDs was repeated 3 times for each range of emission maxima: 520−530 nm, 530−540 nm, and 540−550 nm.

Fluorescent Labeling of BSA. BSA fluorescent labeling was performed according to the standard approach using RBITC.[26] RBITC (9.1 μmol) in 0.5 mL of DMF was added to the solution of BSA (7.5 μmol) in 3 mL of 50 mM phosphate buffer at pH 8.0. The mixture was stirred for 16 h at room temperature. The mixture was then ultracentrifuged (with 50 kDa MWCO) in order to remove the main part of low-molecular weight components. Then, BSARhodB was defatted in accordance with the standard protocol[27] and purified on a PD-10 desalting column. Thin layer chromatography (TLC) was performed on silica-gel plates (eluent $CHCl_3$/methanol 3:1). The concentration of the labeled protein was estimated spectrophotometrically (ε = 108000 $L \cdot M^{-1} \cdot cm^{-1}$ at 554 nm).[28] Thermal denaturation of BSARhodB was performed in 25 mM phosphate buffer at 70 °C for 1 h.

QD−Protein Complex Formation: Kinetics of the Process. Defatting of BSA and BSARhodB was carried out immediately before each experiment in accordance with the standard protocol.[27] The solution of BSARhodB (0.25 mM) was added to the solution of CdSe/ZnSMPA QDs (with an emission wavelength in one of the ranges mentioned above) in 25 mM phosphate buffer at pH 8.0 until the final protein/QD mole ratio was 1:1 (the final complex concentration was about 5 μM). Fluorescence spectra of the mixture were collected every 20 min starting from the moment of component mixing in a 1 cm quartz cuvette cell, while the samples were excited at 450 nm. After 2−3 h, when the fluorescence intensity ratio of QDs and rhodamine B became constant, three aliquots of 200−300 μL each were isolated for further analyses by dynamic light scattering (DLS) and gel electrophoresis. Similar procedures were performed with native BSA and thermally denatured BSARhodB.

Physicochemical Properties of Complexes: Measuring by DLS, Gel Electrophoresis, and pH-Sensitivity. Measurements of the hydrodynamic diameter of particles were conducted in 25 mM phosphate buffer at pH 8.0. Ten-fold aliquot dilution was

performed in an embedded cuvette of Nanotrac Ultra. An average hydrodynamic diameter of the particles and their size distribution were estimated by four successive measurements, each 60 s long.

Gel electrophoresis was done using 1.4% agarose gel in 60 mM Tris-glycine buffer (pH 8.3) for 50 min at 90 V. The fluorescent bands were detected on the UV transilluminator (Vilber Lourmat, France) with an excitation at 365 nm.

The influence of pH on formation and the properties of the complexes were studied in 25 μM phosphate buffers with pH between 6.0 and 12.0. The procedure of the sample preparation was similar to the one described above. The fluorescence of the solutions was visualized by UV irradiation in glass vials at 312 nm.

Titration of CdSe/ZnSMPA−BSARhodB Complexes with Oleic Acid. *Calculation of FRET Parameters.* A predefined amount of oleic acid was thoroughly dispersed in 25 mM phosphate buffer with pH 8.0 at a moderate temperature (40−50 °C) until an almost transparent 0.1 mM solution was obtained. A little acidulation of the solution was compensated by the addition of NaOH. Oleic acid solutions with 10 and 1 μM concentrations were prepared by successive dilutions of the 0.1 mM stock solution.

The QD/protein complexes prepared as described above were titrated directly in a spectrophotometric cuvette cell without light. Oleic acid solutions with concentrations ranging from 10 nM to 5 μM were used. The interval between the injections was 15−20 min (the time when the fluorescence intensity became constant).

The following equation was used to evaluate the FRET effectiveness:

$$E = (F_{AD}/F_A - 1)\cdot OD_A/OD_D \quad (1)$$

where F_{AD} and F_A are the fluorescence intensities of A in the complex and in the free state, respectively, and OD_A and OD_D are the optical densities of A and D at an excitation wavelength, respectfully.[7]

Thus, when the system passes from the state with E_0 to E_i, it is valid to use the F_AD_i/F_DA_i to F_AD_0/F_DA_0 ratio as a relative efficiency variation value. Consequently, when $F_AD_i/F_DA_i > F_AD_0/F_DA_0$ the standard value of normalized correlation (R_I) may be expressed as follows:

$$R_I = [(F_AD_i/F_DA_i)/(F_AD_0/F_DA_0) - 1] \quad (2)$$

RESULTS AND DISCUSSION

FRET Theory and the Main Principles of FRET-Based Sensor Systems Adjusting. FRET efficiency (E) is a key parameter of FRET-based sensors. Relative changes of E could be monitored by the determination of intensity of emission ratio A to D (R_I) as described in the Experimental Procedures section. The formation of a complex between donor and acceptor gives rise to the FRET effect; therefore, the variable R_I changes from ~0, when $r \gg R_0$ (in solution), to the final value, which is more than 0 and depends on r and R_0. The use of QDs as energy donors enables the variation of both r and R_0 parameters. On the one hand, quantum dots with smaller diameter produce complexes with smaller r values, provided that the mechanism of complex formation does not change with the decrease of particle size. On the other hand, the reduction of QD size leads to the blue shift of an emission peak. This shift results in the change of an overlap with the absorption spectrum of acceptor and accordingly in the

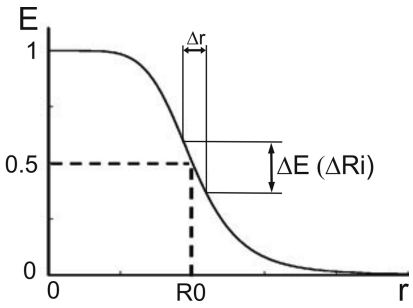

Figure 1. Dependence of the energy transfer efficiency (E) on the distance (r) between D and A. Considerable changes in FRET efficiency (ΔE) occur when r is close to the Förster radius (R_0).

change of R_0. Moreover, the fluorescence quantum yield of donor decreases as the emission peak undergoes a blue shift (closer to 500 nm) because the QD size reduction leads to the relative increase in surface defects. As a result, the value of R_0 decreases. When the aim is to monitor the formation of the D/A complex, then the maximum analytical response will be reached if the FRET efficiency is close to 100%. QDs suitable for this purpose should have small enough size but must at the same time exhibit significant spectral overlap (J) with the absorption spectrum of the acceptor and preferably should have high fluorescence quantum yield.

However, if the goal is to follow the conformational changes inside the complex (changes of r value, namely, Δr), then the analysis of the above equations and the dependence of E on r (see Figure 1) suggest that the maximum changes of E in the D/A system will take place in the case when the original FRET efficiency E_0 is close to 50% (linear part of the curve) and $r \cong R_0$. Thereafter, to reduce the FRET efficiency, it is sufficient to decrease J and (or) the quantum yield of D fluorescence, which can be easily achieved by variation of spectral characteristics of QDs by changing their size.

However, the greatest sensitivity of the FRET system is achieved when the value of r approaches the value of Δr (see Figure 1). Since Δr is constant for a particular protein−ligand system, in the case of BSA approaching 1 nm in diameter,[29] the variation of the r value may also significantly affect the signal change before and after ligand binding. In order to implement and to investigate the above suppositions, it was suggested to use water-soluble CdSe/ZnSMPA QDs of different size as D with emission maximum in the range of 520−550 nm. Defatted BSA fluorescently labeled by rhodamine B residue was suggested to be used as A. BSA was chosen due to the fact that it is a well-characterized protein,[30,31] it binds specific fatty acids effectively,[32,33] and it is readily affordable. Spontaneous formation of MPA coated complexes of CdTe with BSA conjugates has been already described.[8] The stoichiometry of 1:1 has been shown for these complexes by a combination of methods of fluorescence correlation spectroscopy and capillary electrophoresis. In the present study, we used identical particle sizes as well as surface coating. Therefore, we suggested that the QD/protein complex stoichiometry was also 1:1, which will be discussed in detail below.

The estimation of the FRET parameters (J, R_0) in the final CdSe/ZnSMPA−BSARhodB system was based on the assumption that $\kappa \cong 2/3$, as has been described earlier.[34] As far as κ^2 can vary from 0 to 4, this estimation is considered to be quite conventional.[13] The data are shown for the comparison in Table 1. When the emission maximum shifts from 520 to 550

Table 1. Calculated Parameters of FRET (J and R_0) for CdSe/ZnSMPA−BSARhod Complexes with Different QD PL Band Position[a]

	520−530 nm	530−540 nm	540−550 nm
$J \cdot 10^{13}$ ($cm^{-6} \cdot mmol^{-1}$)	3.3	4.5	5.7
R_0 (Å)	38	45	53
QY (%)	2−7	10−15	12−20
E (%)	35	55	40
calculated ranges of QD diameters (Å)	29−33	31−37	33−41
r (Å)	42	44	57
Δr (Å)	−0.6	−0.6	−0.8

[a] Average distance r between fluorophores and its decrease Δr after adding an appropriate amount of oleic acid was calculated from corresponding estimation of FRET efficiencies.

nm, the growth of the J value takes place, as the acceptor absorption maximum (Rhod B residue) shifts to 554 nm. In addition, the fluorescence quantum yield of QDs becomes higher with the increase in the emission wavelength, which leads to the growth of R_0 as well as of the FRET efficiency.

Design and Properties of QD−Protein System. Colloidal CdSe/ZnSMPA nanocrystals were synthesized in three steps in accordance with the published protocols[23] with some modifications. In particular, the use of HMDST as a precursor instead of elementary sulfur resulted in hydrophobic CdSe/ZnS QDs with lower fwhm values of the peak and larger fluorescence quantum yield (data not shown). The use of ammonia saturated methanol solution as a precipitating agent at the last step made it possible to reduce the amount of undesired CdSe/ZnSMPA aggregates. Furthermore, the size distribution of the particles determined by the DLS method (see Supporting Information) was narrower and closer to the calculated value than that of QDs precipitated in the presence of other bases. It is worth mentioning that the use of repeated precipitation cycles led to a higher reproducibility of experiments and to a practically complete absence of hydrophobic ligands in the final CdSe/ZnSMPA solution. Fluorescence quantum yields of the obtained QDs were relatively high (up to 20%) for nanocrystals with a longer emission wavelength (close to 550 nm). In the case of QDs with emission at 520−530 nm, these values were noticeably lower (down to 2%) and were poorly reproducible due to the increase in the amount of defects on the surface of nanocrystals.[35]

BSA equimolarly modified by the Rhod B residue was suggested as an acceptor of the FRET-system. Modification was performed as described above[26] with RBITC (see Figure 2A). The obtained product was additionally defatted according to the standard protocol[27] and then separated from low molecular weight compounds by gel-filtration. Absorption spectrum of the conjugate in the region of 400−600 nm (see Figure 3A) almost completely matched the spectrum of a free dye in water solution, indicative of the insignificant influence of BSA on the optical properties of Rhod B. Thereby, spectral properties of D and A (see Figure 3A) met all the requirements of a FRET-system.

Several approaches have already been described to obtain QD−BSA complexes.[8,36−38] As a rule, chemical modification of BSA or large excess of the protein was required. It is known that the chemical modification frequently leads to the decrease or to the total loss of biological activity; hence, this approach was excluded from the current work. The use of a large excess of protein is not only wasteful but also causes difficulties in the following determination of the stoichiometry of BSA−QD complex. Therefore, in this study the approach of QD−BSA

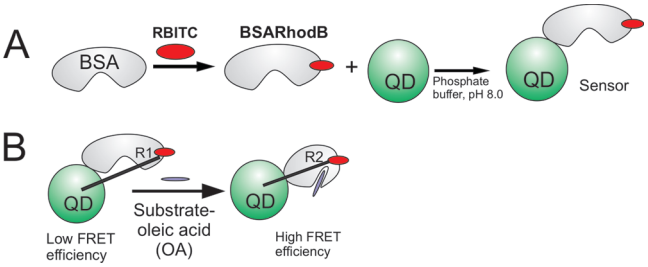

Figure 2. Principal scheme of the antioleic acid sensor. (A) Scheme of complex formation between QDs CdSe/ZnSMPA and rhodamine B (RBITC) labeled BSA. (B) A model of conformational changes in the CdSe/ZnSMPA−BSARhod complex leading to the decrease of distance between D and A coupled with the increase of FRET efficiency.

1:1 self-assembly was used. This principle has already been described for MPA coated CdTe QDs.[8] The present approach is rather simple and indeed leads to the desired effect, which is corroborated by a number of experimental data shown below.

The process of complex formation was controlled after the change of the fluorescence spectrum of the solution at the excitation wavelength 450 nm (Rhod B absorption minimum) after mixing up the components directly in a fluorometer cell. The value R_I was used as a quantitative parameter. In this case, FDA was determined at the CdSe/ZnSMPA emission maximum of QDs and FAD at the emission maximum of the dye (581 nm). Significant decrease of r value in the QD−BSARhod complex relative to its value in solution of components leads to a substantial increase in the FRET efficiency and increase in the R_I value, respectively. Figure 3B shows the typical time dependence of R_I corresponding to complex formation. The curve reaches its plateau after 1.5−3 h, depending on the type of QDs. QDs with larger emission wavelength and, respectively, of larger size, form complexes at a higher speed, which can be explained by a greater amount of MPA ligands on their surface, which results in stronger electrostatic interactions with the protein.

The QD−BSA complexes were characterized using several independent methods. The estimation of the hydrodynamic diameter of particles before and after complex formation indicates that the complex size is close to the sum of the sizes of original QDs and BSA (see Supporting Information). The initial components and the obtained complexes were analyzed by agarose gel electrophoresis (see Figure 4A). It is known that the mobility of a substance depends on the size of particles as well as on their charge. Upon QD−protein complex formation, both parameters change, making it difficult to predict the gel mobility

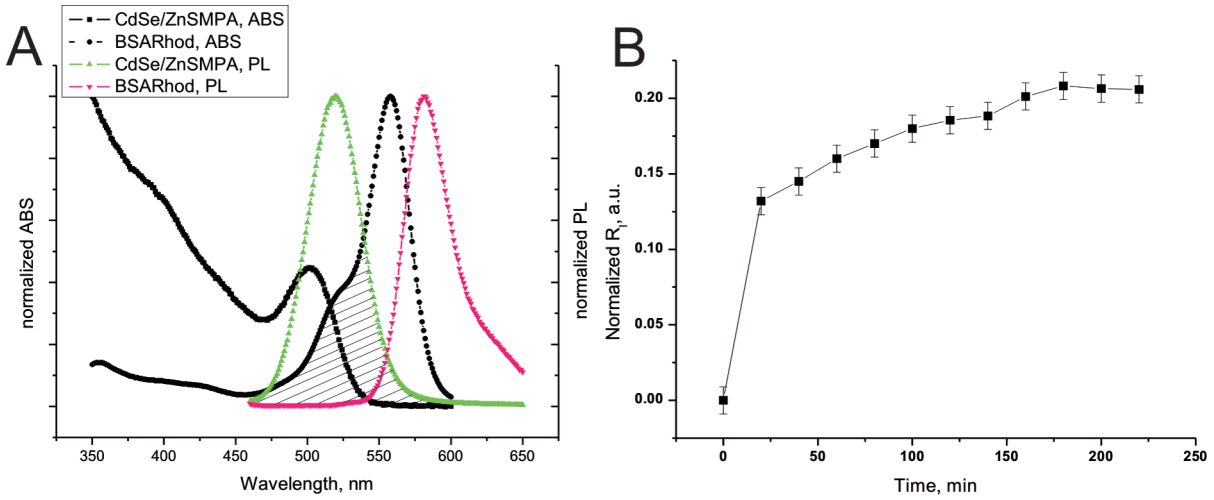

Figure 3. (A) Representative spectral properties of QDs (520 nm < λem < 550 nm) and the BSARhod conjugate. The shaded area corresponds to the integral overlap (J) between the donor emission (green line) spectrum with the acceptor absorption spectrum (dashed black line). (B) Kinetics of CdSeZnSMPA−BSARhod complex formation (QDs λem = 522 nm).

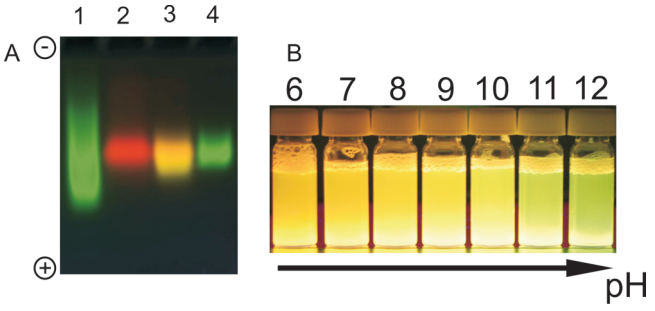

Figure 4. Fluorescence of different QDs and their complexes with BSA. (A) Agarose gel electrophoresis of different fluorescent probes (1.4% agarose gel, Tris−glycine buffer (pH 8.3), 90 V). (1) CdSe/ZnSMPA, (2) BSARhod, (3) CdSe/ZnSMPA−BSARhod complex, and (4) CdSe/ZnSMPA−BSA complex. Excitation wavelength was 365 nm. (B) Visual changes in the fluorescence of the CdSe/ZnSMPA−BSARhod complex at different pH values as indicated under vials. Excitation wavelength was 312 nm.

change. Nevertheless, the results show that the mobility of the initial protein is rather similar to the mobility of complexes CdSe/ZnSMPA−BSA and CdSe/ZnSMPA−BSARhodB, while the mobility of free QDs is substantially higher. No difference in the mobility of free protein and its complex with QDs was detected. This observation might be explained by partial neutralization of the positive charges of the protein through interaction with the surface of QDs. The increase in particle size compensates the increase in negative charge of the QD−BSA complex. However, it is obvious that free QDs interact notably with the gel matrix, which leads to the tailing effect on the electrophoregram. The obtained data are in good agreement with the data earlier observations[36] and additionally demonstrate the higher stability of QD−protein complexes compared to free QDs.

We suggest that the stoichiometry of complexes QD/BSA was 1:1. It can be confirmed by the following facts: in accordance with the synthetic procedure, QDs and BSA were mixed in the ratio of 1:1; no free QDs were observed on the electrophoregram. This suggestion was also corroborated by the DLS measurements of the particles' hydrodynamic diameters before and after complex formation (see Supporting Information, Figure S1). No free QDs or BSA were detected by DLS after 3 h of exposure.

The electrostatic forces are considered to be the main type of interactions in the formation of the complexes.[8] Since the charges depend not only on the ionic strength but also on the solution pH, we studied the influence of pH on QD−BSA complex stability. For this purpose, fluorescence spectra of CdSe/ZnSMPA/BSARhodB mixtures 1:1 were recorded in phosphate buffers with various pH values. The notable change of the R_I value was found at a pH range between 10 to 11 (data not shown). The decrease in the FRET efficiency with the increase in pH was so evident that it could be detected visually (see Figure 4B). The intensive change of R_I from pH 10 to 11 confirms that lysine and arginine (pK_B in polypeptide chain 10−11[39]) are responsible for the formation of positive charges on the BSA molecule. The deprotonation of these basic residues obviously leads to the loss of a positive charge on the surface of the protein followed by the dissociation of the complex and, consequently, by the reduction of FRET efficiency. Thus, the obtained system might be used as a fluorescent pH sensor in the pH range of 9−12.

Sensor Properties of Complexes with Respect to the Natural BSA Ligand Oleic Acid. Present work suggests a simple sensor based on the principle of self-assembly of QDs and fluorescent labeled protein in a complex retaining the original specificity of the protein. Conformational change in BSA upon oleic acid binding can be used to design FRET sensors.[29] In the present study, we determined the change in spectral properties of the complex (CdSe/ZnSMPA−BSARhodB (see Figure 2B)) depending of the change in BSA structure upon oleic acid binding.

The changes in emission spectra of the CdSe/ZnSMPA−BSARhodB complex during titration with oleic acid solution are shown in Figure 5A (the example of QDs with emission maximum in the range of 530−540 nm). Relative increase in the emission intensity of A and decrease of this value for D means the increase in FRET efficiency. This indicates that conformational changes occur in the system that are more likely expressed in the decrease of the distance r between D and A, as the contribution of κ is proportional to that of r in the power of three. The quantitative parameters of

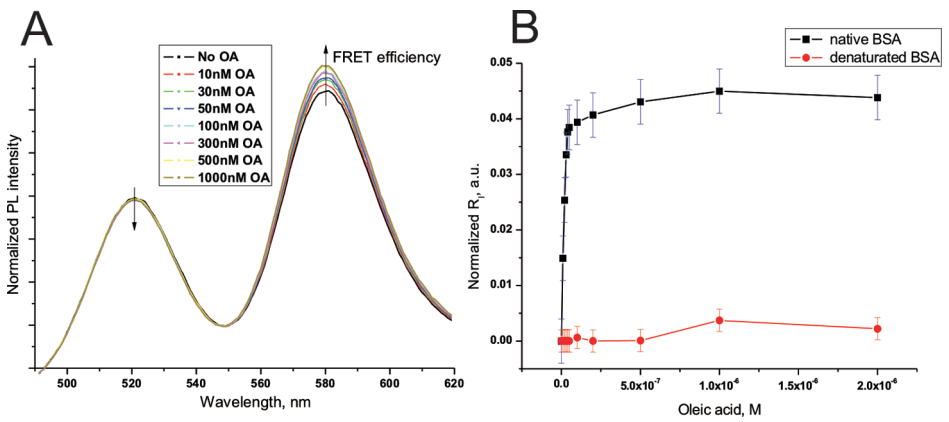

Figure 5. (A) PL spectra of the CdSe/ZnSMPA−BSARhod complex at different OA concentrations. (B) Titration curve based on PL spectra changes at different oleic acid concentrations for CdSe/ZnSMPA−BSARhod (native) and CdSe/ZnSMPA−BSARhod (denatured) complexes.

titration data are also represented in Figure 5B (the results of three independent experiments with the QD emission maximum in the range of 540−550 nm). The analysis of the curve suggests that the most abrupt changes occur at 10−100 nM of oleic acid and the plateau is reached when oleic acid concentration approaches 1 μM. The concentration of the complexes which actively change their conformation seems to be much lower than their total concentration (5 μM). This hypothesis may be explained by the fact that the modification of BSA with rhodamine B occurs statistically with different $-NH_2$ groups of amino acids and leads to the emerging of various BSARhodB isomers. Further complex formation with QDs can gives rise to different CdSe/ZnSMPA−BSARhodB isomers, wherein the rhodamine B residue can be located on varying distances from the QD center. As it was mentioned, the most notable spectral changes must occur when $r \cong R_0$. For this reason, complexes with E values close to 50% were selected (see Table 1). It should be taken into consideration that this value can as well be an average for the isomeric complexes with high (close to 100%) and low (close to 0%) values of the FRET efficiency and should be taken into account with caution. Nevertheless, the sensor allowed the detection of oleic acid reproducibly at 10 nM concentration, which is comparable to the systems reported earlier.[19]

The specificity of spectral changes was confirmed using the thermally denatured BSARhodB. It was shown that such complexes in similar conditions (see Figure 5B) did not exhibit any noticeable response to the addition of oleic acid. As was shown earlier, thermal denaturation induces irreversible changes in the protein tertiary structure and the loss of high affinity to fatty acids.[32] Therefore, it was demonstrated here that the natural ligand specificity of BSA is necessary for the performance of the nanosensor.

Logical continuation of the research was the comparison of the analytical response of the CdSe/ZnSMPA−BSARhodB systems with QDs, their emission maxima being appreciably different. The titration with oleic acid was carried out as described above for CdSe/ZnSMPA complexes with the following fluorescence emission ranges: 520−530 nm, 530−540 nm, and 540−550 nm. Average relative values of analytical response (normalized maximum R_I values) for these complexes are shown in Figure 6. The greatest averaged value of the analytical response of this system was observed in case of the blueshifted QDs (520−530 nm), which may be related to the fact that other conditions being almost equal, the R_0 value of the CdSe/ZnSMPA−BSARhodB system is lower than that of the others (38 Å) and thereby closer

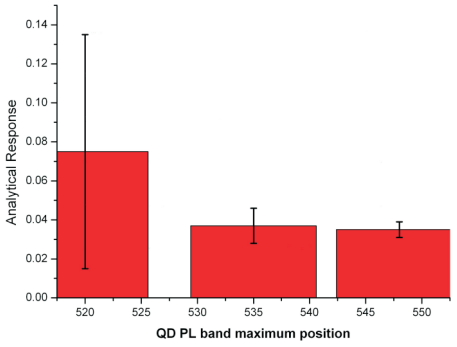

Figure 6. Relative analytical response of complexes with different QDs (from left to right, λem was 520−530 nm, 530−540 nm, and 540−550 nm).

to the Δr value. Consequently, the change in distance r after oleic acid binding will induce a greater effect on FRET efficiency and R_I. However, it was observed that QDs with an emission in this range exhibit low reproducibility of the fluorescence quantum yield (see Table 1). As a result, data scattering was quite significant. However, QDs with emission in a longer wavelength region showed less response, but the results were well reproducible.

In conclusion, the described approach is promising for the design of nanosensors based on QDs and proteins. The methodology and synthetic part of the present work come to the standard modification of the protein with an organic dye and the synthesis of the appropriate QDs (see Figure 2). The adjustment of QD spectral properties and size gives an opportunity to produce nanosensors with maximum sensitivity to an analyte. We hope that the derived model due to its simple tunability could become a universal approach for the production of sensors with specificities to various analytes. In further investigations, we intend to demonstrate the universal applicability of the present design by using other ligand-specific proteins.

■ ASSOCIATED CONTENT

Supporting Information. Distribution of the particle hydrodynamic size by dynamic light scattering and corresponding average sizes. This material is available free of charge via the Internet at http://pubs.acs.org.

dx.doi.org/10.1021/bc100133u |*Bioconjugate Chem.* 2011, 22, 338–345

AUTHOR INFORMATION

Corresponding Author
*Phone: 7-496-212-76-37. E-mail: dezh@mail.ru.

ACKNOWLEDGMENT

We express our gratitude to Professor Jonathan S. Lindsey from Glaxo Distinguished University (Country) for kindly providing the PHOTOCHEMCAD software for the calculation of FRET parameters. This work was supported by grant RFBR No. 08-02-01142-a from Russian Foundation for Basic Research.

REFERENCES

(1) Lakowicz, J. R. (2006) *Principles of Fluorescence Spectroscopy*, 3rd ed., Springer, Berlin, Germany.

(2) Mulrooney, R. C., Singh, N., Kaur, N., and Callan, J. F. (2009) An "off−on" sensor for fluoride using luminescent CdSe/ZnS quantum dots. *Chem. Commun. (Cambridge, U. K.) 6*, 686–688.

(3) Freeman, R., Li, Y., Tel-Vered, R., Sharon, E., Elbaz, J., and Willner, I. (2009) Self-assembly of supramolecular aptamer structures for optical or electrochemical sensing. *Analyst (Cambridge, U. K.) 134*, 653–656.

(4) Boeneman, K., Mei, B. C., Dennis, A. M., Bao, G., Deschamps, J. R., Mattoussi, H., and Medintz, I. L. (2009) Sensing caspase 3 activity with quantum dot-fluorescent protein assemblies. *J. Am. Chem. Soc. 131*, 3828–3829.

(5) Callan, J. F., De Silva, A. P., Mulrooney, R. C., and Mc Caughan, B. (2007) Luminescent sensing with quantum dots. *J. Inclusion Phenom. Macrocyclic Chem. 58*, 257–262.

(6) Medintz, I. L., and Mattoussi, H. (2009) Quantum dot-based resonance energy transfer and its growing application in biology. *Phys. Chem. Chem. Phys. 11*, 17–45.

(7) Kang, J. S., Piszczek, G., and Lakowicz, J. R. (2002) Enhanced emission induced by FRET from a long-lifetime, low quantum yield donor to a long-wavelength, high quantum yield acceptor. *J. Fluoresc. 12*, 97–103.

(8) Shao, L., Dong, C., Sang, F., Qian, H., and Ren, J. (2009) Studies on interaction of CdTe quantum dots with bovine serum albumin using fluorescence correlation spectroscopy. *J. Fluoresc. 19*, 151–157.

(9) Gao, X., Chan, W. C. W., and Nie, S. (2002) Quantum-dot nanocrystals for ultrasensitive biological labeling and multicolor optical encoding. *J. Biomed. Opt. 7*, 532–537.

(10) Walling, M. A., Novak, J. A., and Shepard, J. R. E. (2009) Quantum dots for live cell and In Vivo imaging. *Int. J. Mol. Sci. 10*, 441–491.

(11) Willard, D. M., Carillo, L. L., Jung, J., and Orden, A. V. (2001) CdSe-ZnS quantum dots as resonance energy transfer donors in a model protein-protein binding assay. *Nano Lett. 1*, 469–474.

(12) Pinaud, F., King, D., Moore, H., and Weiss, S. (2004) Bioactivation and cell targeting of semiconductor CdSe/ZnS nanocrystals with phytochelatin-related peptides. *J. Am. Chem. Soc. 126*, 6115–6123.

(13) Laib, S., and Seeger, S. (2004) FRET studies of the interaction of dimeric cyanine dyes with DNA. *J. Fluoresc. 14*, 187–191.

(14) Fagot-Campagna, A., Balkau, B., Simon, D., Warnet, J., Claude, J., Ducimetiered, P., and Eschwegea, E. (1998) High free fatty acid concentration: an independent risk factor for hypertension in the Paris Prospective Study. *Int. J. Epidemiol. 27*, 808–813.

(15) de Jong, R. T., Serne, E. H., Ijzerman, R. G., de Vries, G., and Coen, D. A. (2004) Free fatty acid levels modulate microvascular function: relevance for obesity-associated insulin resistance, hypertension, and micro-angiopathy. *Diabetes 53*, 2873–2882.

(16) Nawrocki, A. R., and Scherer, P. E. (2004) The delicate balance between fat and muscle: adipokines in metabolic disease and musculoskeletal inflammation. *Curr. Opin. Pharmacol. 4*, 289–294.

(17) Westphal, S., Gekeler, G. H., Dierkes, J., Wieland, H., and Luley, C. (2002) A free fatty acid tolerance test identifies patient with coronary artery disease among individuals with a low conventional coronary risk profile. *Heart Vessels 16*, 79–85.

(18) Bergen, W. G., and Mersmann, H. J. (2005) Comparative aspects of lipid metabolism: Impact on contemporary research and use of animal models. *J. Nutr. 135*, 2499–2502.

(19) Bartolome, A., Bardliving, C., Rao, G., and Tolosa, L. (2005) Fatty acid sensor for low-cost lifetime-assisted ratiometric sensing using a fluorescent fatty acid binding protein. *Anal. Biochem. 345*, 133–139.

(20) Susanto, F., Humfeld, S., and Reinauer, H. (1986) Measurement of oleic acid in human plasma by isotope dilution mass spectrometry. *Chromatographia 21*, 693–696.

(21) Gagne, S., Crane, S., Huang, Z., Li, C. S., Bateman, K. P., and Levesque, J. (2007) Rapid measurement of deuterium-labeled long-chain fatty acids in plasma by HPLC-ESI-MS. *J. Lipid Res. 48*, 252–259.

(22) Chen, X., Dong, X., and You, J. (2010) Determination of free fatty acids from soil by LC−MS with fluorescence detection and atmospheric pressure chemical ionization identification. *Chromatographia 72*, 171–175.

(23) Capek, R. K., Lambert, K., Dorfs, D., Smet, P. F., Poelman, D., Eychmuller, A., and Hens, Z. (2009) Synthesis of extremely small CdSe and bright blue luminescent CdSe/ZnS nanoparticles by a prefocused hot-injection approach. *Chem. Mater. 21*, 1743–1749.

(24) Yu, W. W., Qu, L., Guo, W., and Peng, X. (2003) Experimental determination of the extinction coefficient of CdTe, CdSe, and CdS nanocrystals. *Chem. Mater. 15*, 2854–2860.

(25) Grabolle, M., Spieles, M., Lesnyak, V., Gaponik, N., Eychmuller, A., and Resch-Genger, U. (2009) Determination of the fluorescence quantum yield of quantum dots: suitable procedures and achievable uncertainties. *Anal. Chem. 81*, 6285–6294.

(26) Staiano, M., Scognamiglio, V., Mamone, G., Rossi, M., Parracino, A., Rossi, M., and D'Auria, S. (2006) Glutamine-binding protein from Escherichia Coli specifically binds a wheat gliadin peptide. 2. Resonance energy transfer studies suggest a new sensing approach for an easy detection of wheat gliadin. *J. Proteome Res. 5*, 2083–2086.

(27) Chen, R. F. (1967) Removal of fatty acids from serum albumin by charcoal treatment. *J. Biol. Chem. 242*, 173–181.

(28) Mchedlov-Petrosyan, N. O., and Kholin, Y. V. (2004) Aggregation of rhodamine B in water. *Russ. J. Appl. Chem. 77*, 414–422.

(29) Soetewey, F., Rosseneu-Motreff, M., Lamote, R., and Peeters, H. (1972) Size and shape determination of native and defatted bovine serum albumin monomers. *J. Biochem. 71*, 705–710.

(30) Hsia, J. C., Wong, L. T., Tan, C. T., Er, S. S., Kharouba, S., Balaskas, E., Tinker, D. O., and Feldhoff, R. C. (1984) Bovine serum albumin: characterization of a fatty acid binding site on the N-terminal peptic fragment using a new spin-label. *Biochemistry 23*, 5930–5932.

(31) Hamilton, J. A., Era, S., Bhamidipati, S. P., and Reed, R, G. (1991) Locations of the three primary binding sites for long-chain fatty acids on bovine serum albumin. *Proc. Natl. Acad. Sci. U.S.A. 88*, 2051–2054.

(32) Parks, J. S., Cistola, D. P., Small, D. M., and Hamilton, J. A. (1983) Interactions of the carboxyl group of oleic acid with bovine serum albumin: a 13C NMR study. *J. Biol. Chem. 258*, 9262–9269.

(33) Bojesenl, I. N., and Bojesen, E. (1994) Binding of arachidonate and oleate to bovine serum albumin. *J. Lipid Res. 35*, 770–778.

(34) Dennis, A. M., and Bao, G. (2008) Quantum dot-fluorescent protein pairs as novel fluorescence resonance energy transfer probes. *Nano Lett. 8*, 1439–1445.

(35) Loef, R., Houtepen, A. J., Talgorn, E., Schoonman, J., and Goossens, A. (2009) Study of electronic defects in CdSe quantum dots and their involvement in quantum dot solar cells. *Nano Lett. 9*, 856–859.

(36) Bucking, W., Massadeh, S., Merkulov, A., Xu, S., and Nann, T. (2010) Electrophoretic properties of BSA-coated quantum dots. *Anal. Bioanal. Chem. 396*, 1087–1094.

(37) Xie, H., Liang, J., Zhang, Z., Liu, Y., He, Z., and Pang, D. (2004) Luminescent CdSe-ZnS quantum dots as selective Cu2+ probe. *Spectrochim. Acta, Part A 60*, 2527–2530.

(38) Liang, J. G., Xie, H. Y., Ai, X. P., He, Z. K., and Pang, D. W. (2004) A novel method for the selective determination of silver (I) ion. *Chin. Chem. Lett. 15*, 1319–1322.

(39) Andre, I., Linse, S., and Mulder, F. A. A. (2007) Residue-specific pKa determination of lysine and arginine side chains by indirect 15N and 13C NMR spectroscopy: application to apo calmodulin. *J. Am. Chem. Soc. 129*, 15805–15813.